Energy, Mines and Resources Canada | Énergie, Mines et Ressources Canada

CANMET

Canada Centre for Mineral and Energy Technology | Centre canadien de la technologie des minéraux et de l'énergie

ULTRASONIC INSPECTION OF STEPWISE CRACKING

D.K. Mak
Non-Destructive Testing Section

February 1983

AUG 19 1983

MICROMEDIA

This document is an unedited interim report prepared primarily for submission and discussion at a meeting. It does not represent final opinion or policy of the Canada Centre for Mineral and Energy Technology (CANMET)

Ce document est un rapport provisoire non-révisé et rédigé principalement pour fins de discussion et de documentation lors d'une réunion. Il ne représente nulle part l'expression définitive de l'opinion du Centre canadien de la technologie des minéraux et de l'énergie (CANMET)

16 pp

ENERGY RESEARCH PROGRAM
PHYSICAL METALLURGY RESEARCH LABORATORY
REPORT: ERP/PMRL 83-10(TR)

PHYSICAL METALLURGY RESEARCH LABORATORIES
REPORT ERP/PMRL 83-10(TR)

ULTRASONIC INSPECTION OF STEPWISE CRACKING

by

D.K. Mak*

ABSTRACT

Twenty-seven coupons of linepipe exposed to H_2S environments were inspected for stepwise cracking (SWC) by ultrasonic C-scan. Their crack-area ratios (CAR) were measured and compared with the square of crack-length ratios (CLR) deduced from examination of their metallographic sections. Sixty per cent of the results from the two methods agree within experimental error.

Although some of the experimental errors in CLR are larger than 100%, the error of CAR is estimated to be about 14%. It is felt that ultrasonic inspection gives a more accurate evaluation of stepwise cracking.

---

*Research Scientist, Physical Metallurgy Research Laboratories, Energy Research Laboratories, CANMET, Energy, Mines and Resources Canada, Ottawa

LABORATOIRES DE LA MÉTALLURGIE PHYSIQUE
RAPPORT ERP/PMRL 83-10(TR)

CONTRÔLE PAR ULTRASONS DES FISSURES EN GRADINS

par

D.K. Mak*

RÉSUMÉ

Vingt-sept éprouvettes de tubes exposés à des milieux chargés de H_2S ont été inspectées au moyen de la méthode du contrôle par ultrasons (présentation C), en vue de détecter des fissures en gradins. Les rapports des surfaces des fissures (CAR) de ces éprouvettes ont été mesurés et comparés au carré des rapports des longueurs des fissures (CLR) qui avaient été déduits de l'examen de leurs sections métallographiques. Soixante pour cent des résultats de ces deux méthodes concordent à l'intérieur de la marge d'erreur expérimentale.

Quelques-unes des erreurs expérimentales de la méthode du CLR sont supérieures à 100 p. 100, mais l'erreur moyenne du CAR est estimée à environ 14 p. 100. On pense donc que le contrôle par ultrasons permet d'obtenir une évaluation plus exacte des fissures en gradins.

---

*Chercheur scientifique, Laboratoires de recherche en métallurgie physique, Laboratoires de recherche sur l'énergie, CANMET, Énergie, Mines et Ressources, Ottawa.

INTRODUCTION

The susceptibility of linepipe to cracking in hydrogen sulphide (H_2S) environments has been investigated at the Physical Metallurgy Research Laboratories (PMRL). In particular, stepwise cracking (SWC) due to hydrogen damage associated with general corrosion in the presence of H_2S has been examined by G.J. Biefer (1). Metal coupons were removed from pipes and exposed for a certain period of time to H_2S-saturated synthetic sea water. They were then sectioned and examined for cracks. Crack-length ratio (CLR) representing the amount of cracking in the rolling plane can thus be measured. It is felt that the coupons should also be scanned ultrasonically to assess SWC. This method is capable of showing the hydrogen-damaged area in plan. It is the purpose of the current project to make such measurements.

EXPERIMENTAL PROCEDURE

The experiment was performed in an immersion tank at Alcan International Ltd. in Kingston, Ontario. The ultrasonic flaw detector used was a Type SIJ Reflectoscope S80 manufactured by the Sperry Division of Automation Industries Inc. A 5.0 MHz FM (medium focus) transducer, J374, was used. The transducer is 3/4 in. diam and has a focal length of 95 mm in water, with a beam size 2.3 mm in diam at the focus.

Two dummy steel coupons with material that was the same as the real coupons, were prepared. One of these contained flat-bottomed holes and the other side-drilled holes. They were immersed in a water tank with Na_2CrO_4 solution (0.12 g/l H_2O) to inhibit rusting of the inspected metal pieces.

The ultrasonic search unit was adjusted such that the transducer focused on a 1/16 in. diam flat-bottomed hole located at 1/2-thickness of the dummy coupon. As the velocity of sound in steel is four times that in the water, and the coupon is about 13 mm thick, the distance of the water path between the transducer and the surface of the coupon is 69 mm in practice. The gate width on the S80 was adjusted such that the gate started right after the front-wall reflection and ended before the back-wall reflection; the threshold of the gate was set at 30% of the screen height. The gain on the echo amplitude was adjusted such that the size of the 1/16 in. diam hole recorded on XY recorder paper was the same as its physical size. The appropriate gain

control was found to be 28 dB. The pulse repetition rate was 1.2 KHZ, slow enough for echos from the second pulse not to overlap with those from the first.

The pipeline coupons were put inside the immersion tank. They were inspected by the ultrasonic C-scanning search unit at a speed of 14 cm/s, a hard copy of the results of the inspection being produced at the same time.

RESULTS

Stepwise cracking (SWC) was observed in most of the 27 coupons. The results are produced in Fig. 1-5. The cracks are shown as dark area and were estimated to correspond to the real cracks by an error of no more than 10%.

Crack Area Ratio (CAR), defined as

$$\frac{\text{Total area of cracks}}{\text{Top surface area of coupon}}$$

can be measured by a planimeter or an image analysing computer. The latter method was eventually chosen because it is less time-consuming. The results are shown in Table 1 as CAR_{raw}. It should be noted because of the finite beam size the exterior boundary of the white areas in Fig. 1-5 is larger than that of the top surface area of the coupon. By measuring the dimensions of the white area and those of the coupon, it was found that the CAR_{raw} needed to be multiplied by a factor of 1.3 to yield the correct CAR. Also, the dark areas on the CD coupons do not reveal cracks but show only the edges of the coupons. This was verified by manual inspection of the coupons in the immersion tank at PMRL. After correcting for these systematic errors, the error of measuring the CAR using image analysis was estimated to be about 10%. Combining this error with that contributed from ultrasonic inspection brings the total error of the measured CAR to about 14%. Table 1 shows the CAR values for the coupons tested.

DISCUSSION

Metal coupons can be sectioned and examined for SWC (2). Crack-length ratio was measured for each section examined, as in the study by Biefer et al (3).

Crack Length Ratio (CLR) = $\frac{\Sigma \ell}{L}$

where ℓ = crack length

L = section length (Fig. 6)

The average CLR value was calculated from nine sections, the standard deviation being taken as the error (Table 5). Some of the errors were larger than 100%. This is not surprising as one coupon can have one section that is crack-free whilst another section can be filled with cracks. This is illustrated in Table 2-4 which lists individual CLR taken from each section of three types of pipe coupons which had a high crack density. This variation of CLR from section to section can also be observed in Fig. 1-5.

CAR can be compared with CLR^2 (Table 5). Sixty per cent of their results agree within experimental error. Their values are also compared graphically for 2 of the 3 types o pipe coupons mentioned above (Fig. 7-8). A straight line with a slope of 1 is drawn on each figure. If CAR = CLR^2, the points will lie on the straight line. It should be pointed out that the CLR is not measured on the same coupon as the CAR is calculated, but from neighboring coupons. Furthermore, the definition of CLR implies that it can be larger than 1 (see Fig. 6) while CAR is always less than 1. It will thus seem that CLR^2 will be always larger than CAR. As Table 5 and Fig. 7-8 show, this is not so. It is particularly not true for the Z coupons where CAR is much larger than CLR^2. A possible explanation could be that ultrasonic inspection has a higher sensitivity than microscopic examination of metallographic sections and can locate finer cracks and discontinuities, thus leading to CAR values larger than CLR^2 values. This can be tested by recording results of the ultrasonic C-scan on a coupon at different threshold level setting of the gate. The results can be compared with those deduced from microscopic examination of many different metallographic sections of the same coupon.

CONCLUSIONS

The standard deviation of crack-length ratio of stepwise cracking (SWC) in metallographic sections of pipeline coupons can be larger than 100%. Crack-area ratio deduced from ultrasonic inspection is estimated to have an

error of about 14%. It appears that ultrasonic inspection is a more accurate method for determining crack ratios for SWC than metallographic methods.

ACKNOWLEDGEMENTS

We thank Alcan International Ltd., Kingston for use of their automatic ultrasonic system. We would like to acknowledge Mr. Yvon Levesque of Alcan for his help with experimental work, Mr. Jack Newbury for preparation of dummy steel coupons and Dr. M.T. Shehata for image analysis measurements.

REFERENCES

1. Biefer, G.J. Materials Performance 21, 19; 1982.

2. Fichera, M.J. Division Report ERP/PMRL 81-51(INT); CANMET, Energy, Mines and Resources Canada; 1981.

3. Biefer, G.J., Fichera, M. and Selwyn, J. Division Report ERP/PMRL 81-39(TR); CANMET, Energy, Mines and Resources Canada; 1981.

Table 1. Crack area ratio of pipe coupons in tests in H_2S - saturated synthetic sea water. CAR_{raw} is measured using the image analysing computer method. It is corrected for the finite beam effect to yield CAR. Both CAR_{raw} and CAR have an error of about 14%.

Coupon No.	Location in pipe	CAR_{raw}	CAR
AB-3W	Across weld	0.04	0.052
AB-28	Parent, 90° from weld	<0.01	<0.01
AB-53	Parent, 180° from weld	<0.01	<0.01
AE-3W	Across weld	0.34	0.44
AE-28	Parent, 90° from weld	0.65	0.85
AE-53	Parent, 180° from weld	0.77	1.0
AG-3W	Across weld	0.11	0.14
AG-28	Parent, 90° from weld	<0.01	<0.01
AG-53	Parent, 180° from weld	0.13	0.17
CA-17W	Across weld	0.11	0.14
CA-28	Parent, 90° from weld	0.15	0.20
CA-53	Parent, 180° from weld	0.06	0.08
CB-3W	Across weld	0.02	0.026
CB-30	Parent, 90° from weld	0.49	0.64
CB-53	Parent, 180° from weld	0.53	0.69
CC-3W	Across weld	0.17	0.22
CC-28	Parent, 90° from weld	0.07	0.09
CC-53	Parent, 180° from weld	0.015	0.02
CD-3W	Across weld	0.0	0.0
CD-28	Parent, 90° from weld	0.0	0.0
CD-53	Parent, 180° from weld	0.0	0.0
CE-3W	Across weld	0.0	0.0
CE-28	Parent, 90° from weld	0.0	0.0
CE-53	Parent, 180° from weld	0.0	0.0
Z-3W	Across weld	0.08	0.10
Z-28	Parent, 90° from weld	0.40	0.52
Z-53	Parent, 180° from weld	0.41	0.53

Table 2. CLR in tests in H_2S - saturated synthetic sea water on pipe AE. Data taken from private communication with G. Biefer.

Coupon No.	Location in Pipe	Section No.	CLR x100%
AE-1W	Across	1	29.8
	weld	2	1.4
		3	23.1
AE-5W	Across	1	32.0
	weld	2	17.2
		3	31.7
AE-10W	Across	1	0.7
	Weld	2	11.9
		3	69.8
AE-26	Parent, 90°	1	33.2
	from weld	2	66.2
		3	98.3
AE-34	Parent, 90°	1	76.3
	from weld	2	38.1
		3	87.3
AE-42	Parent, 90°	1	40.3
	from weld	2	62.9
		3	62.0
AE-51	Parent, 180°	1	127.8
	from weld	2	33.7
		3	40.3
AE-59	Parent, 180°	1	10.3
	from weld	2	77.5
		3	104.2
AE-67	Parent, 180°	1	91.9
	from weld	2	86.6
		3	66.2

Table 3. CLR in tests in H_2S - saturated synthetic sea water on pipe CB. Data taken from Biefer et al (3).

Coupon No.	Location in Pipe	Section No.	CLR x100%
CB-1W	Across weld	1	0
		2	0
		3	0
CB-5W	Across weld	1	0
		2	0
		3	0
CB-10W	Across weld	1	7.8
		2	0
		3	4.3
CB-26	Parent, 90°	1	38.8
	from weld	2	13.6
		3	23.1
CB-34	Parent, 90°	1	42.6
	from weld	2	70.5
		3	34.5
CB-42	Parent, 90°	1	114.6
	from weld	2	41.8
		3	24.9
CB-51	Parent, 180°	1	77.0
	from weld	2	61.1
		3	166.8
CB-59	Parent, 180°	1	63.7
	from weld	2	108.0
		3	78.9
CB-67	Parent, 180°	1	90.6
	from Weld	2	52.4
		3	63.2

Table 4 CLR in tests in H_2S saturated synthetic sea water on pipe Z. Data taken from Biefer et al (3).

Coupon No.	Location in Pipe	Section No.	CLR x100%
Z-1W	Across weld	1	0
		2	0
		3	0
Z-5W	Across weld	1	0
		2	0
		3	0
Z-10W	Across weld	1	0
		2	0
		3	0
Z-26	Parent, 90°	1	35.2
	from weld	2	31.7
		3	24.5
Z-34	Parent, 90°	1	48.7
	from Weld	2	34.9
		3	13.5
Z-42	Parent, 90°	1	16.8
	from weld	2	14.5
		3	54.5
Z-51	Parent, 180°	1	58.7
	from weld	2	15.2
		3	45.7
Z-59	Parent, 180°	1	28.0
	from weld	2	48.2
		3	26.3
Z-67	Parent, 180°	1	0
	from Weld	2	0
		3	14.9

Table 5 Comparison of CAR with CLR^2. CLR is the average of nine sections. Values of CLR are taken from Biefer et al (3) and from private communication with G. Biefer. Data of CA-across weld is from private communication with G. Biefer.

Coupon No.	Location in Pipe	CLR	CLR^2	CAR
AB	Across weld	0.19 ± 0.25	0.035 ± 0.095	0.052 ± 0.007
	Parent, 90° from weld	0.054 ± 0.062	0.003 ± 0.007	<0.01 ± 0.001
	Parent, 180° from weld	0.074 ± 0.10	0.005 ± 0.007	<0.01 ± 0.001
AE	Across weld	0.24 ± 0.21	0.059 ± 0.101	0.44 ± 0.06
	Parent, 90° from weld	0.63 ± 0.23	0.39 ± 0.28	0.85 ± 0.12
	Parent, 180° from weld	0.71 ± 0.37	0.50 ± 0.53	1.0 ± 0.1
AG	Across weld	0.26 ± 0.30	0.07 ± 0.16	0.14 ± 0.02
	Parent, 90° from weld	0.007 ± 0.016	0.00004 ± 0.00022	<0.01 ± 0.001
	Parent, 180° from weld	0.035 ± 0.091	0.001 ± 0.006	0.17 ± 0.02
CA	Across weld	0.20 ± 0.13	0.04 ± 0.05	0.14 ± 0.02
	Parent, 90° from weld	0.26 ± 0.23	0.07 ± 0.12	0.20 ± 0.03
	Parent, 180° from weld	0.40 ± 0.23	0.16 ± 0.18	0.08 ± 0.01
CB	Across weld	0.013 ± 0.028	0.0002 ± 0.0007	0.026 ± 0.004
	Parent, 90° from weld	0.45 ± 0.31	0.20 ± 0.28	0.64 ± 0.09
	Parent, 180° from weld	0.85 ± 0.35	0.72 ± 0.60	0.69 ± 0.10
CC	Across weld	0.037 ± 0.078	0.0014 ± 0.0058	0.22 ± 0.03
	Parent, 90° from weld	0.058 ± 0.045	0.0033 ± 0.0052	0.09 ± 0.01
	Parent, 180° from weld	0.21 ± 0.15	0.04 ± 0.06	0.02 ± 0.002
CD	Across weld	0.0 ± 0.0	0.0 ± 0.0	0.0 ± 0.0
	Parent, 90° from weld	0.0 ± 0.0	0.0 ± 0.0	0.0 ± 0.0
	Parent, 180° from weld	0.0 ± 0.0	0.0 ± 0.0	0.0 ± 0.0
CE	Across weld	0.0 ± 0.0	0.0 ± 0.0	0.0 ± 0.0
	Parent, 90° from weld	0.0 ± 0.0	0.0 ± 0.0	0.0 ± 0.0
	Parent, 180° from weld	0.0 ± 0.0	0.0 ± 0.0	0.0 ± 0.0
Z	Across weld	0.0 ± 0.0	0.0 ± 0.0	0.10 ± 0.01
	Parent, 90° from weld	0.31 ± 0.15	0.09 ± 0.09	0.52 ± 0.0
	Parent, 180° from weld	0.26 ± 0.21	0.07 ± 0.11	0.53 ± 0.07

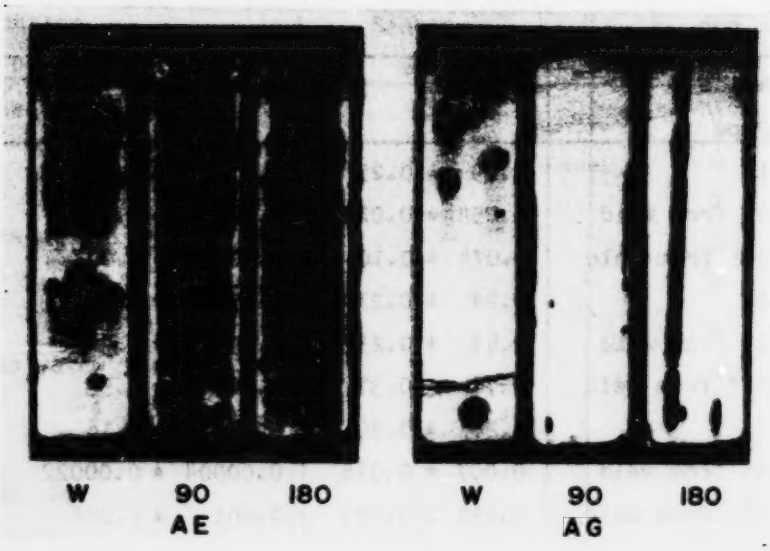

Fig. 1. Results obtained using ultrasonic C-scanning on coupons AE and AG. (neg 7574)

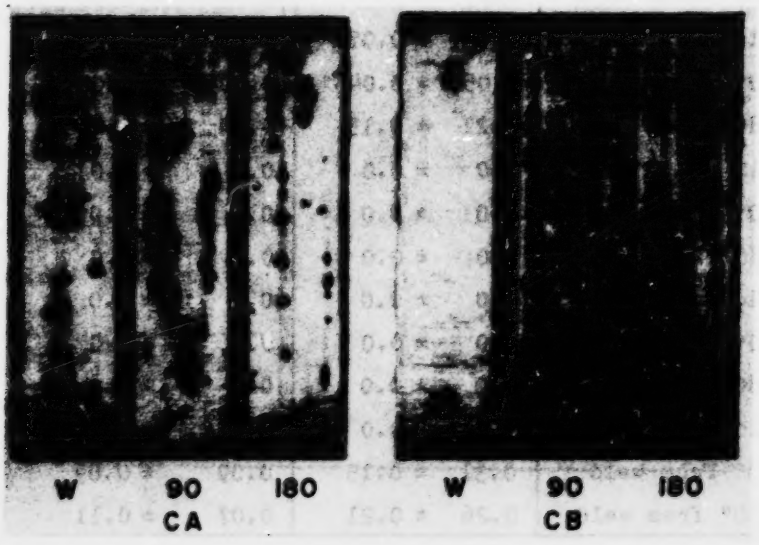

Fig. 2. Results obtained using ultrasonic C-scanning on coupons CA and CB. (neg 7575)

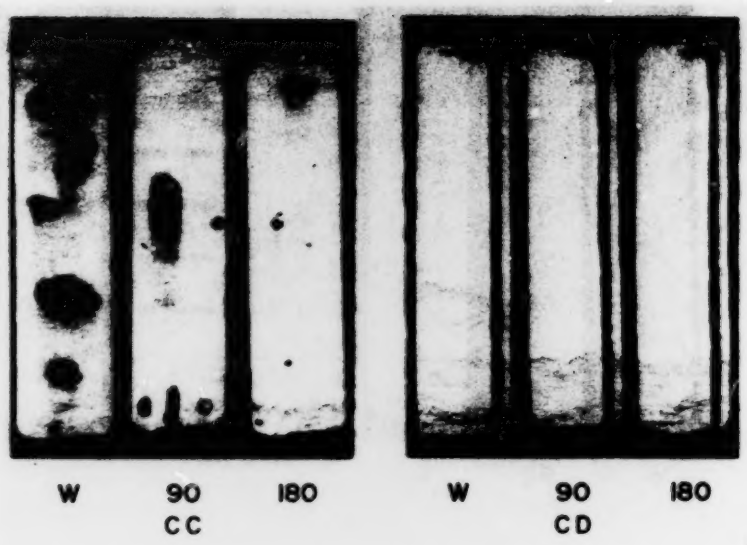

Fig. 3. Results obtained using ultrasonic C-scanning on coupons CC and CD. (neg 7577)

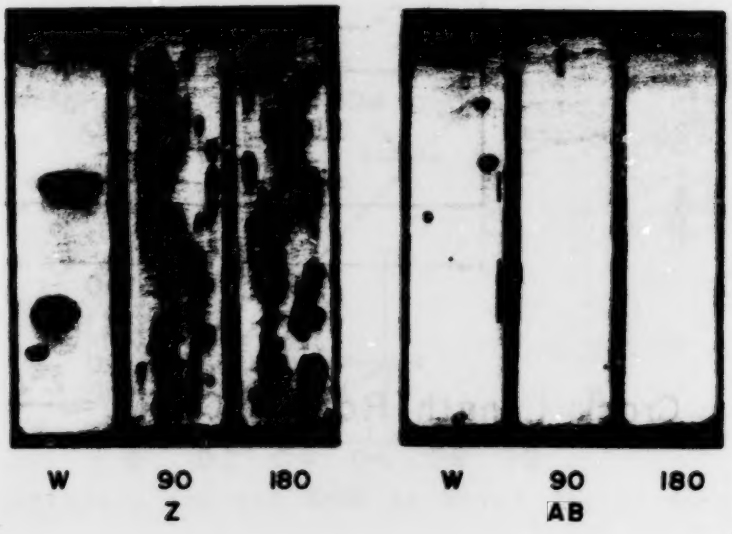

Fig. 4. Results obtained using ultrasonic C-scanning on coupons Z and AB. (neg 7576)

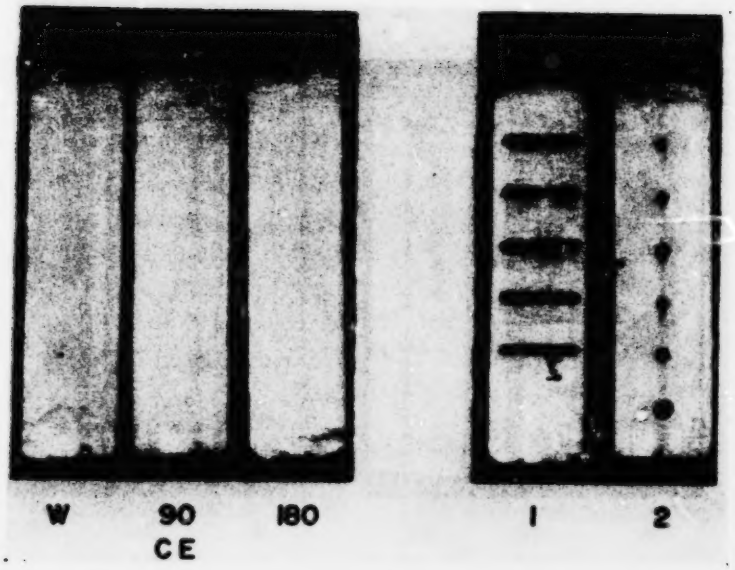

Fig. 5. Results obtained using ultrasonic C-scanning on coupons CE and dummy coupons 1, 2. Dummy coupon 1 contains side-drilled holes. Dummy coupon 2 contains flat-bottomed holes. (neg 7573)

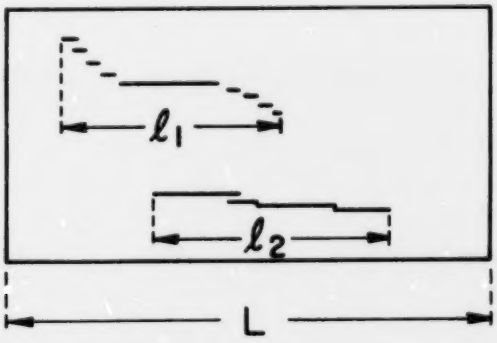

$$\text{Crack Length Ratio (CLR)} = \frac{\Sigma \ell}{L}$$

Fig. 6. Crack length ratio is used for the quantitative evaluation of SWC in metallographic section. (neg 7911)

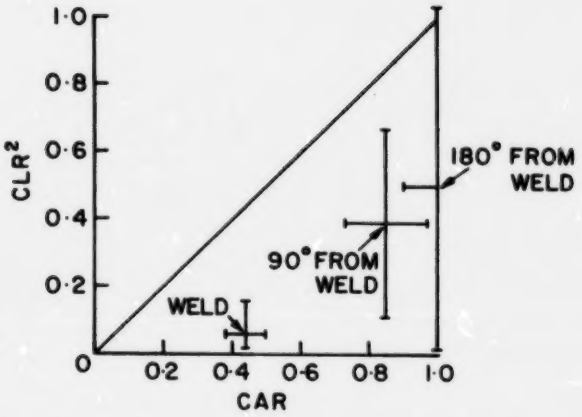

FIG. 7 Comparison of CAR with CLR^2 for line pipe coupon AE

Fig. 7. Comparison of CAR with CLR^2 for linepipe coupon AE. (neg 7912)

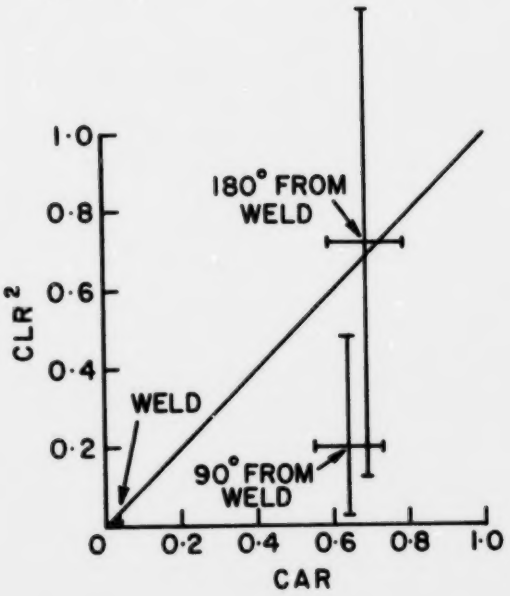

Fig. 8. Comparison of CAR with CLR^2 for linepipe coupon CB. (neg 7913)